ELSEVIER

Available online at www.sciencedirect.com

ScienceDirect

Energy Procedia 00 (2015) 000–000

Energy Procedia

www.elsevier.com/locate/procedia

9th International Renewable Energy Storage Conference, IRES 2015

The CellFlux Storage Concept for Increased Flexibility in Sensible Heat Storage

Christian Odenthal, Wolf-Dieter Steinmann*, Markus Eck

German Aerospace Center (DLR), Institute of Technical Thermodynamics, Pfaffenwaldring 38, 70569 Stuttgart

Abstract

Packed beds using air at atmospheric pressure as heat transferring medium are the most cost effective systems for sensible heat storage. The basic idea of the CellFlux concept is to apply this concept also for liquid and/or pressurized primary HTFs by the introduction of an intermediate working fluid cycle. A heat exchanger is used for transferring energy between the primary HTF and the intermediate air cycle which eventually transfers the energy to a packed bed. The CellFlux concept can be implemented by using standard components. Essential is the minimization of efficiency losses resulting from the circulation of the air as well as the heat transfer processes within the heat exchanger and the storage volume. Some example cost estimations for the heat exchanger are given. The feasibility of the CellFlux concept has been proven by a pilot scale test facility operated at a maximum temperature of 380 °C and 100 kW. A novel approach promising further cost reductions has been applied by realizing a horizontal flow direction. Results from the theoretical and experimental analysis of the CellFlux concept will be presented. Distinctive for the CellFlux concept is the flexibility regarding working fluid (thermal oil, molten salt, pressurized water, CO_2), temperature range (0-800 °C), power (kW-multi MW) and storage medium (rocks, clinker bricks, concrete). This allows a wide range of applications. An example for application in combined heat and power will be given.

Peer-review under responsibility of EUROSOLAR - The European Association for Renewable Energy.

Keywords: CellFlux; Sensible Heat; Thermal Energy Storage; Power to Heat; Packed Bed; Regenerator;

* Corresponding author. Tel.: +49 711 6862 785; fax: +49 711 6862 747.
E-mail address: wolf.steinmann@dlr.de

Peer-review under responsibility of EUROSOLAR - The European Association for Renewable Energy.

1. Motivation for the CellFlux concept

The CellFlux storage concept is aiming for significant cost reductions in sensible heat thermal energy storage applications such as CSP. The idea standing behind the CellFlux concept is decoupling power and capacity as in the 2-Tank-molten salt concept and simultaneously utilizing the advantage of solid low cost sensible heat storage material. Possible materials are concrete or clinker bricks or a packed bed consisting of basalt rocks, which has been proven to withstand temperatures around 600°C [1]. Any of these materials can often be found or produced locally, which reduces transportation costs and increases the local share.

Nomenclature

ΔT_{log}	logarithmic temperature difference	/ K
T, TC	temperature	/ °C
C	costs	/ €
c	specific costs	/ €/kWh
h	height	/ m
g	gravity	/ m/s^2
ρ	density	/ kg/m^3
c_p	specific heat capacity	/ J/kgK
$\dot{Q}$	thermal power	/ W
P	mechanical power	/ W
$\dot{m}$, mdot	mass flow	/ kg/s
$\dot{V}$	volume flow	/ m^3/s
t	time	/ s
HEX	heat exchanger	
stor, S	storage	
tot	total	
spec	specific	
disch	discharge	
buoy	buoyancy	
H / C	hot / cold	

Since most liquid primary heat transferring fluids (HTF) cannot be brought into direct contact with such storage material, a gaseous intermediate working fluid must be applied. Air as working fluid (WF) is suggested, but other gases such as CO_2 are possible alternatives too. Heat is transferred by a finned tube heat exchanger from the liquid primary HTF to the gaseous WF. The WF is kept in an enclosed loop and conveyed by a fan. The working principle of a complete CellFlux storage module is illustrated in Fig. 1. The separation of primary HTF and WF by the heat exchanger enables a wide flexibility in possible further applications where alternative primary HTFs such as molten salt or compressed CO_2 can be applied. Furthermore, if the storage system operates at a high temperature level, electricity might be used as a heat source as well.

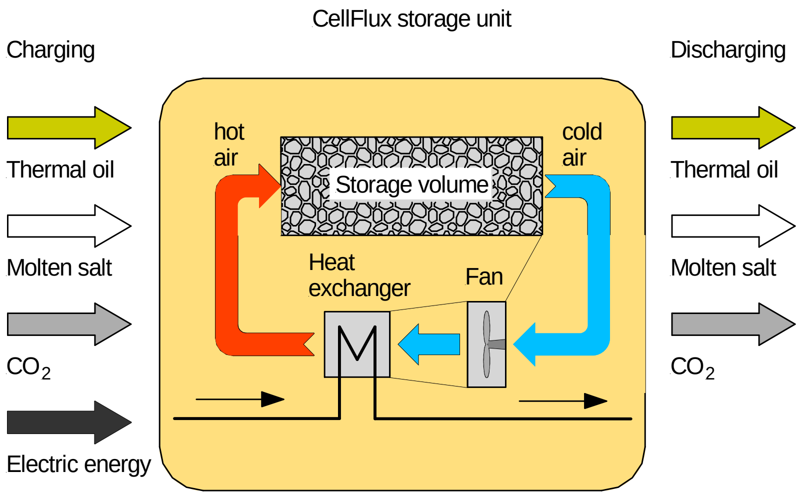

Fig. 1: Basic concept of CellFlux storage module

Besides its low costs, further advantages of the concept are the assembly out of standard components, the utilization of non-corrosive materials, no possible freezing of working fluids, ambient pressure level and low safety risks.

2. Cost Estimation for various CellFlux modules

Due to the poor volumetric heat capacity of gases, parasitic losses as well as higher capital costs through larger heat transfer surfaces are subject to optimization. Crucial element of such optimization is the heat exchanger. Fig. 2 shows calculated steel masses for a finned tube liquid-air heat exchanger with 10 MW thermal power. For the sizing of the heat exchanger the procedure described in [1] has been implemented in Matlab. Hitec HTS as primary working fluid is assumed here since it allows higher operating temperatures but similar results with other liquid HTFs can be expected. The results are grouped in three different operating temperature ranges, the first (H390-L290) operating between 390°C inlet temperature and an exit temperature of 290°C of the primary HTF. This would be suitable for thermal oil based CSP applications. The second group (H510 L310) would be suitable for a molten salt based power plant operating at higher temperatures. For the third group (H510 L210) a lower exit temperature of the HTF is taken into account. Within each group three different logarithmic temperature differences ΔT_{log} are considered. Since the heat capacity flow rates $\dot{m} \cdot c_p$ on both sides of the heat exchanger are the same, the logarithmic temperature difference equals the effective temperature difference ΔT_{eff} between primary HTF and working fluid (WF). ΔT_{log} is varied between 10, 15 and 20 Kelvin. For each of these logarithmic temperature differences four different heat exchangers are sized, having different parasitic losses to overcome air and liquid side pressure losses. The parasitic losses are varied between 36, 72, 144 and 288 kW. Considering 14 necessary CellFlux modules for a power plant having 50 MW gross electric power (140 MW thermal), these parasitic losses would be 0.5, 1, 2 and 4 MW in total parasitics on both primary HTF and WF side.

As can be seen, increasing the logarithmic (i.e. effective) temperature difference from 10 to 20 Kelvin, significantly reduces the total mass of the heat exchanger to less than half of its mass. Allowing for higher parasitic losses, accompanied by a better heat transfer, similar savings in necessary steel mass can be achieved.

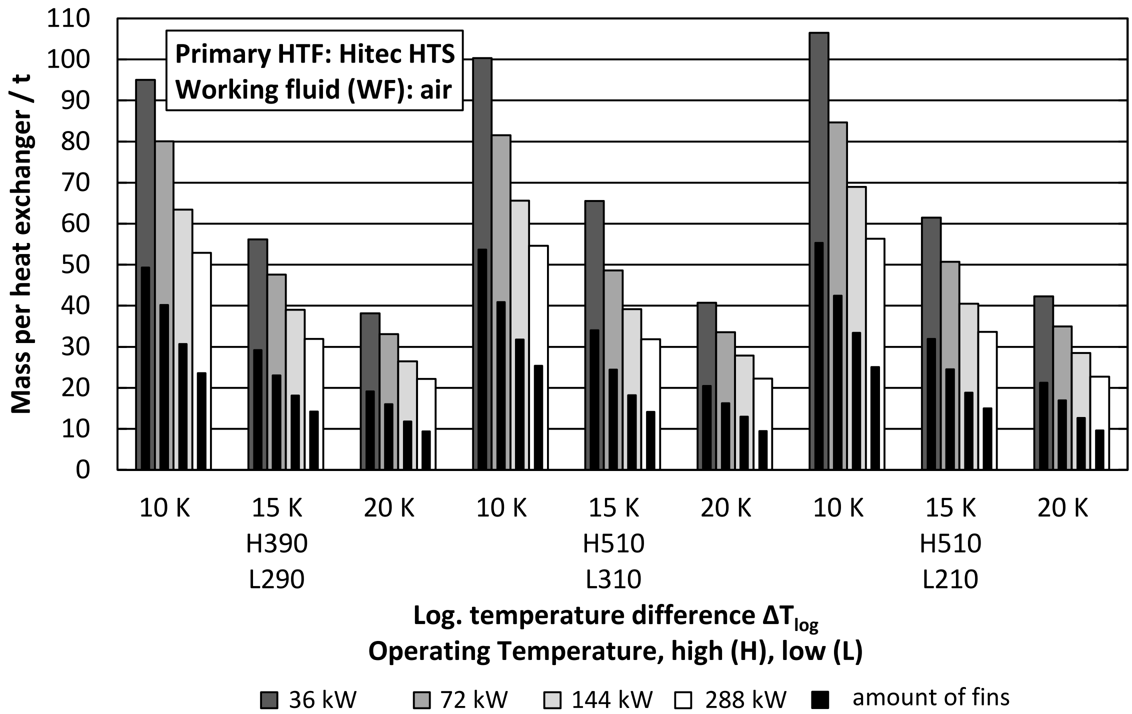

Fig. 2: Necessary steel mass per heat exchanger for a CellFlux module with 10 MW thermal power. Variation of logarithmic temperature difference, operating temperature level and parasitic losses

The total mass of the heat exchanger is considered as an estimate for its total costs, since material costs are the dominating factor and many costs scale linearly with the total mass. If the heat exchanger is manufactured from individually finned carbon steel tubes in G-fin design, a current manufacturing price of 8,000 €/t complete heat exchanger can be assumed [2]. This would be suitable for the H390-L290 case. For parts of the heat exchanger in contact with higher temperatures, laser welded stainless steel tubes should be used. It is assumed that the price is three times higher, yielding 24,000 €/t heat exchanger. Considering the first case (H390-L290) the most expensive heat exchanger with lowest parasitics and ΔT_{log} would cost 760,000 €. Allowing higher parasitics, these costs would drop down to 416,000 €. Higher ΔT_{log} further reduces costs but the simultaneously reduced exit temperature of the primary HTF during discharge has a negative impact on the connected process. One has to bear in mind that the logarithmic temperature difference appears twice, first during charging and secondly during discharging. A ΔT_{log} of 20 Kelvin leads to an absolute temperature of the exiting primary HTF of 350°C during discharging. The output of a typical Clausius-Rankine cycle of said 50 MW gross electric power plant would drop to 42 MW with 10 Kelvin ΔT_{log} and down to only 35 MW with 20 Kelvin ΔT_{log} [3]. In the second case (H510-L310) the most expensive heat exchanger would cost 1.6 Mio € if half of the heat exchanger is manufactured out of more expensive laser welded stainless steel tubes. However, the impact of a higher ΔT_{log} is weaker in this case. A 50 MW power plant [4] would still deliver 45 MW with 10 Kelvin logarithmic temperature difference and about 40 MW with 20 Kelvin ΔT_{log}. A heat exchanger with lowest parasitic losses would cost 656,000 € in this case. Since 14 CellFlux modules are necessary, all prices must be multiplied by 14 to calculate total costs for a 50 MW power plant. An 8 hour storage volume with 140 MW thermal power operating with a temperature difference of 100 Kelvin would need 100,000 tons of basalt or clinker brick storage material, if the utilization of the storage material is around 45% [5]. This value, however, is strongly dependent on the construction and operation strategy of the storage volume but is a realistic estimate. Costs for the storage material lie in the range of 20–30 €/t [6], yielding 2-3 M€. If the storage material can be integrated into a cylindrical storage volume of 10 meter height and 90 m diameter, insulation costs would be another 1 M€. Including a lightweight housing, a concrete foundation and balance of plant, total costs sum up to 6.0 M€. If the temperature difference is doubled (H510 L310) only half of the storage material is necessary. In this case total storage costs of 4.0 M€ are assumed. Table 1 shows estimated total costs from above considerations. Specific costs for storing thermal energy are starting from around 25 €/kWh$_{th}$ and can be as little as only 8 €/kWh$_{th}$. These results must be rated in context with the amount of produced electricity which tends to be higher with increasing specific storage costs. Such a rating must be part of an elaborate cost evaluation of the storage system together with the attached system, i.e. power plant, solar field or industrial process. A direct comparison to the two-tank molten salt system can be drawn for the H390-L290 case with 10 Kelvin ΔT_{log} and lowest parasitics. This case would be a direct substitute of the two tank system but at significantly lower costs of only 15 €/kWh$_{th}$ compared to about 50 €/kWh$_{th}$ for the two tank system.

Table 1: Estimated total costs and power output for selected CellFlux storage units with 140 MW thermal power and a storage capacity of 8 hours

$\boldsymbol{\Delta T_{log}}$		10 Kelvin		20 Kelvin		
Parasitics		0.5	4.0	0.5	4.0	MW
H390 L290	C_{HEX}	10.7	5.9	4.2	2.5	M€
	C_{stor}	6.0				M€
	C_{fan}	0.5				M€
	C_{tot}	17.2	12.4	10.7	9	M€
	$\boldsymbol{c_{spec}}$	15.36	11.07	9.55	8.04	€ / kWh
	$\boldsymbol{P_{el,disch}}$	41.5	38.0	34.5	31.0	MW
H510 L310	C_{HEX}	22.4	12.3	9.8	4.7	M€
	C_{stor}	4.0				M€
	C_{fan}	0.3				
	C_{tot}	26.7	16.6	14.1	9	M€
	$\boldsymbol{c_{spec}}$	23.84	14.82	12.59	8.04	€ / kWh
	$\boldsymbol{P_{el,disch}}$	44.5	41.0	39.5	36.0	MW

3. Horizontal flow direction

As a proof of concept a pilot scale storage unit has been set up at DLR in Stuttgart. For the storage volume a novel approach has been chosen, where air flows through the storage volume horizontally. As indicated in Fig. 3, a vertical flow direction is supported by buoyancy effects, reducing necessary pumping power. On the other hand a support structure is necessary to connect the ductwork to the bottom of the storage volume. If a horizontal flow direction is realized, these additional costs can be avoided.

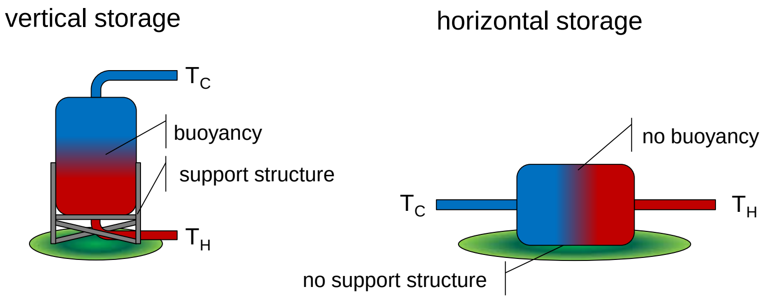

Fig. 3: Comparison of vertical vs. horizontal flow regenerator storage volumes

The question arising from sacrificing the buoyancy effects for lower investment costs is which amount of electric energy could have been saved due to buoyancy effects. The pumping power induced of a volume flow $\dot{V}$ by buoyancy in a chimney of height h and ρ being the hot/cold gas density can be expressed from

$$P_{buoy} = hg\dot{V}\,(\rho_H - \rho_C) \tag{1}$$

For a storage volume having a fixed thermal power $\dot{Q}$, the volume flow depends on the average density $\bar{\rho}$, heat capacity $\bar{c_p}$ and the hot and cold temperature difference $T_H - T_C$

$$\dot{V} = \frac{\dot{Q}}{\bar{\rho} \cdot \bar{c_p} \cdot (T_H - T_C)} \tag{2}$$

Inserting equation (2) in (1) the amount of saved energy by buoyancy can be estimated. For the following calculation a storage volume with 140 MW thermal power is considered with a height of the storage volume of 10 meters and air as WF. It is assumed that the buoyancy effect occurs in the opposite direction inside the heat exchanger as well. Hence, the result is multiplied by two. An electric efficiency of 80% for the fans is assumed. Table 2 shows the results for different operating temperature ranges. The three previously considered cases are marked by black boxes. As can be seen, roughly 50 kW electric energy can be saved, which is comparatively little in contrast to the pumping losses inside the heat exchanger.

Table 2: Electric energy saving potential in kilowatts due to buyancy effects for a 140 MWth storage system with a height of 10 meters and different operating temperature ranges

↓ TC / TH →	300	350	400	450	500	550	600	650	700	750	800
100	71,1	66,6	62,9	59,7	57,2	54,9	52,7	50,3	47,3	43,4	38,3
150	66,5	62,4	59,0	56,3	54,1	52,2	50,3	48,0	45,1	41,1	35,7
200	62,0	58,3	55,4	53,1	51,2	49,7	48,0	46,0	43,0	38,9	33,2
250	57,9	54,7	52,2	50,3	48,9	47,6	46,2	44,2	41,3	36,9	30,8
300	-	51,7	49,6	48,1	47,0	46,0	44,8	42,9	39,8	35,1	28,6
350	-	-	47,7	46,6	45,8	45,0	43,8	41,9	38,6	33,5	26,5
400	-	-	-	45,6	45,0	44,3	43,2	41,0	37,4	31,8	24,1
450	-	-	-	-	44,5	43,9	42,6	40,2	36,1	29,8	21,3
500	-	-	-	-	-	43,3	41,8	38,9	34,2	27,2	17,7

Based on the above considerations, a horizontal flow direction storage volume was designed for the pilot scale plant.

4. Construction of a large scale pilot plant

4.1. Experimental Setup

According to the working principle of the CellFlux concept, the pilot scale plant consists of a primary HTF and a working fluid (WF) loop. The piping and instrumentation diagram (Fig. 4) gives an overview of the plant and distinguishes the two loops by different colors. The primary loop contains thermal oil (Syltherm 800) as HTF which is circulated by an electrical pump. An electric heater with 100 kW thermal power operates as a heat source whereas an air cooler as a heat sink. This part of the pilot plant allows simulating the input/output of a possible process such as a CSP power plant, an industrial process or an Organic-Rankine-Cycle. Two controllable valves allow changing the flow direction of the oil flow. The thermal oil flow is measured by an orifice mass flow meter and the oil temperature is measured at several points inside the heat exchanger and within the primary oil loop.

The working fluid (WF) loop contains air which is conveyed by a fan, having a maximum of 15 kW electrical power and a nominal pressure increase of 3000 Pa. The reason for the comparatively high pressure loss and energy consumption of the fan is mainly due to piping losses. In a large scale plant all components would be moved closer together, minimizing such losses. Since a radial fan is used, a switching valve arrangement changes the flow direction of the air flow. Air temperatures are measured along the flow direction and additionally at multiple points inside the storage volume and the heat exchanger. Pressure losses can be measured over different planes inside the heat exchanger as well as over eleven different planes inside the storage volume.

The insulation of the heat exchanger, the storage volume and the pipes are equipped with additional thermocouples to measure the heat flux through the insulation. By applying Fourier's law, heat losses can be calculated.

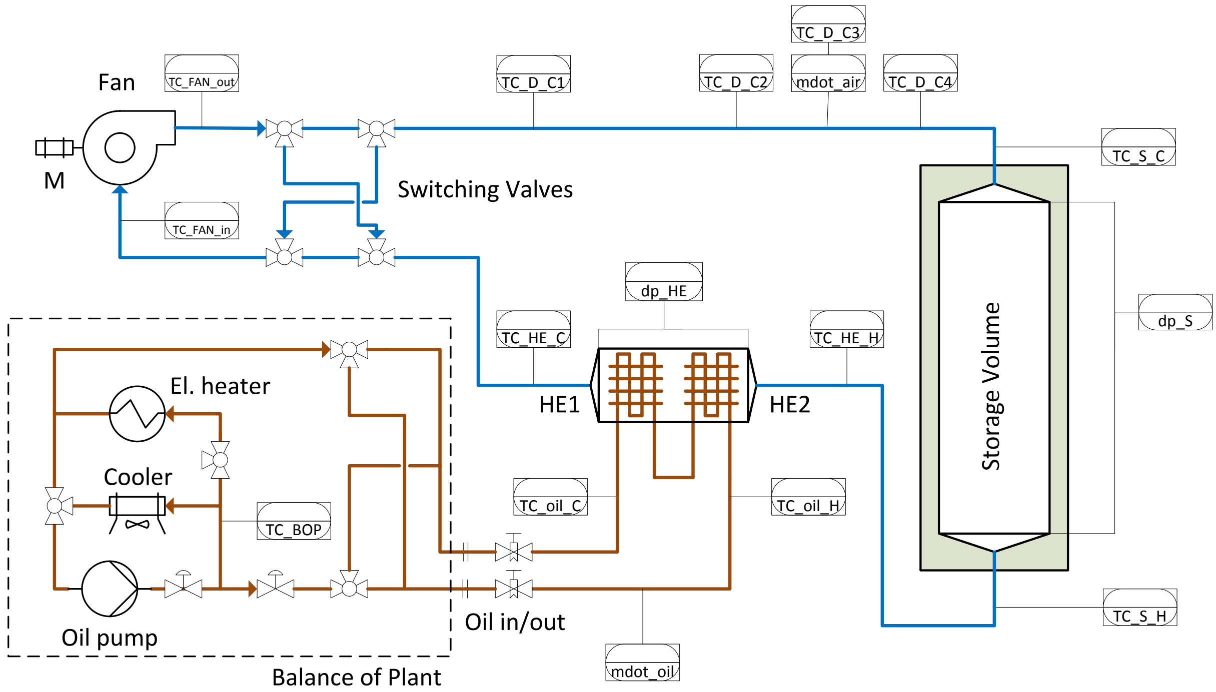

Fig. 4: P&I diagram of the plant with major measurement positions

The storage volume has a total length of 11.9 meters where 0.7 meters on both sides consist of diffusors. The inventory of the storage volume has a length of 10 meters and a frontal area of 2.8m^2. An additional 0.6 meters of the storage volume's flow length on both sides is filled with ceramic saddles for flow stratification. The storage volume is kept in an inner air tight containment. The inner containment itself is located inside an outer container with an insulation of 0.35 meters in between. As storage material standard clinker bricks are utilized [7]. In total there are 40 metric tons of clinker storage material and another 1.4 metric tons of ceramic saddles. Assuming an average heat capacity of the clinker material of 900 J/kgK, the storage capacity of the clinker material is 36 MJ/K or 10 kWh/K. Air temperatures are measured midstream inside the storage volume at every meter down the flow. There are additional thermocouples in an 9x9 pattern at zero, two, five, eight and ten meters flow length, allowing to measure the temperature distribution perpendicular to the flow direction. Fig. 5 shows the position of these thermocouples. The entering and exiting air temperatures are also measured inside the connecting ducts. Static pressure tabs are located at every meter of flow length for measuring the pressure drop over any possible segment of the container.

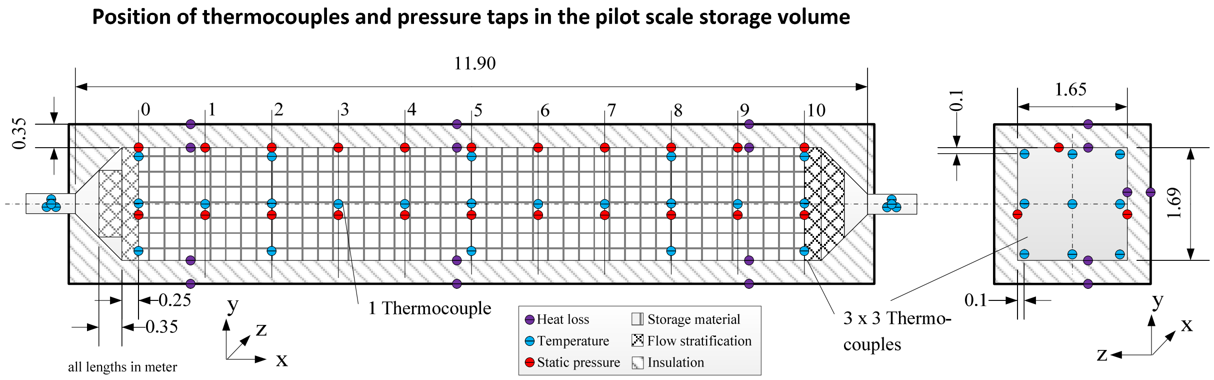

Fig. 5: Position of thermocouples and pressure taps in the storage volume

The next figure shows the frontal view of pilot scale test facility. The primary HTF loop, fan and switching valves are located inside the building. On the right picture the connecting flange, frontal insulation and the ceramic saddle flow stratification of the storage volume have been removed revealing the clinker brick storage material, inner containment and insulation.

Fig. 6: Front view (left) of the pilot scale test facility at DLR and opened outer storage containment revealing the storage material, inner containment and insulation. White circles indicate measurement positions of thermocouples

After commissioning first experiments have been carried out which are described in the next section.

4.2. Experimental results

Some of the experimental results are presented in the next figure. Since the new concept is based on a horizontal flow direction, a homogenous temperature distribution is necessary. Fig. 7 shows the average temperature distribution inside the storage volume when the storage is heated up to a uniform temperature. For averaging, temperatures have been measured over 25 hours. As can be seen the temperature midstream (T_22) is not affected by heat losses to the environment. This will allow investigating the temperature distribution inside the storage volume without considering thermal losses. Temperatures in proximity to the walls and edges show a drop along the flow length. These temperatures have been grouped by different line styles. For example T_21, T_12 and T_23 are temperatures close to the left, top and right wall and all of them show a similar progression. Hence, there is no evidence for a significant maldistribution of the flow. The temperature close to the floor (T_32) experiences higher losses due to the higher conductivity of the floor insulation. TC_S_H and TC_S_C are the mixing temperatures at the hot and cold connection to the storage volume. The transient progression of these temperatures during thermal cycling is shown on the right graph of Fig. 7. In this experiment the storage volume provides a maximum of 60 kW thermal power during discharging at an initial temperature of 370°C falling down to 350°C at the end of discharge.

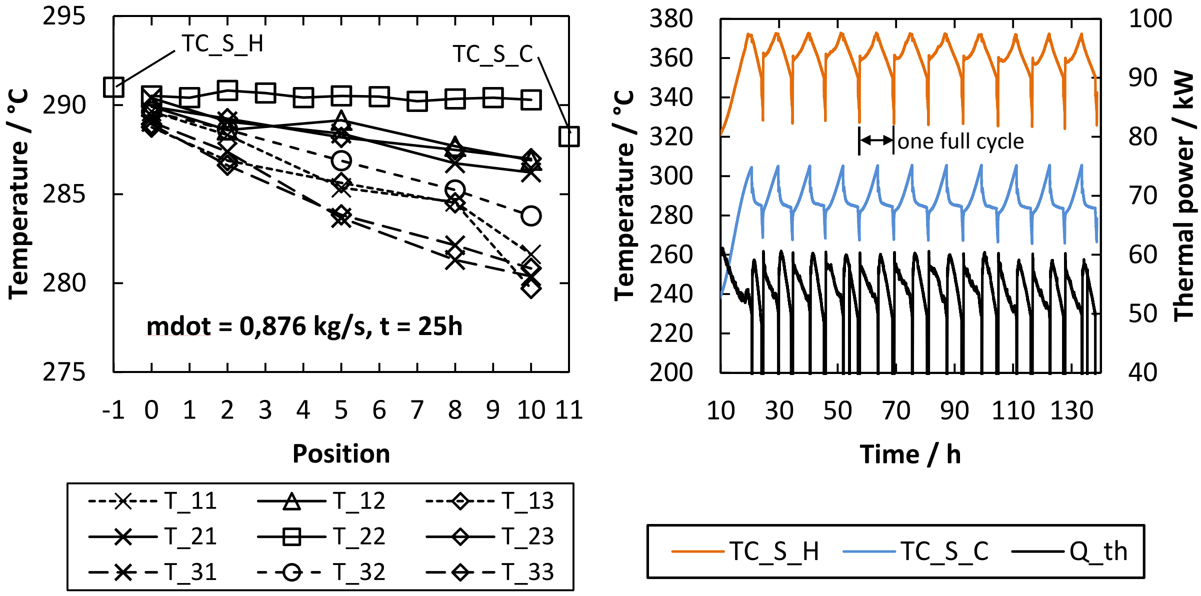

Fig. 7: Average temperature distribution over 25 hours inside the storage volume in flow direction (left). Time variation of the hot and cold air temperatures during thermal cycling (right)

5. Power to combined heat and power

CellFlux can also be used for the storage of surplus electric energy provided for example by renewable energy sources. During charging, the air in the closed air cycle is heated electrically before entering the storage volume. If high temperature storage materials like basalt are used, the maximum temperature of the storage volume is in the range of 800°C. The temperature of the air exiting the storage volume should be in the range of 300°C due to the maximum operation temperature of the fan. The high cyclic temperature difference results in a high volumetric energy density. Compared to the original application of the CellFlux concept in solar thermal power plants, the temperature differences between the air and the working fluid in the heat exchanger of the CellFlux system can be increased, the costs for the heat exchanger can be decreased significantly. The energy provided during discharge is used for operating a combined heat and power system. A steam turbine or an organic Rankine cycle is applied to generate electricity, the remaining thermal energy can be used in industrial processes or for heating applications. Since the system is emission free, it can be built close to the consumer. This concept provides a near term solution for efficient storage of surplus electricity.

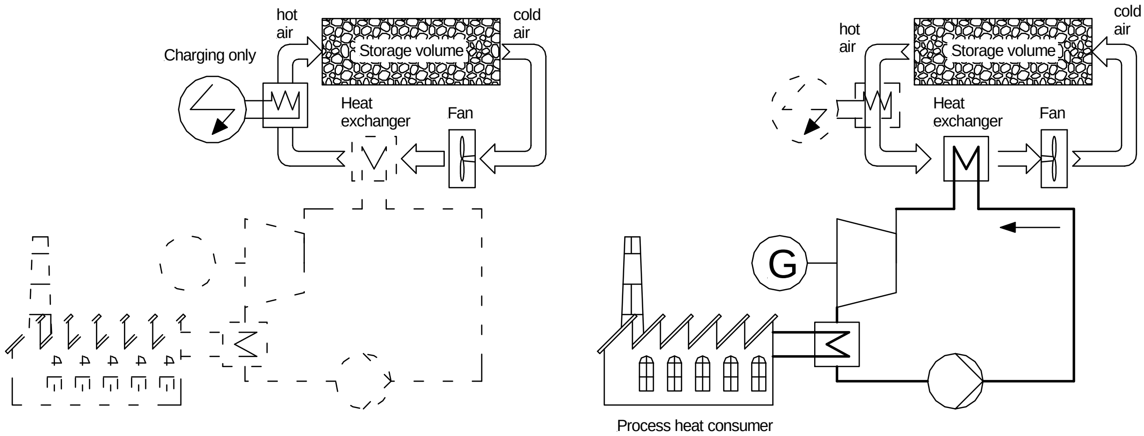

Fig. 8: Combined heat and power based on the CellFlux concept: charging of CellFlux with surplus electric energy (left) and discharge providing both electric energy and heat (right)

Acknowledgements

The authors thank E.ON AG for financing the project as part of the International Research Initiative. Responsibility for the content of this publication lies with the authors.

References

[1] R. K. Shah and D. S. Sekulic, *Fundamentals of heat exchanger design*. 2003.
[2] G. Klein, *Tubetech GmbH, personal communication*. 2014.
[3] R. V. Padilla, “Simplified Methodology for Designing Parabolic Trough Solar Power Plants,” 2011.
[4] M. Seitz, “Thermodynamische Simulation und Optimierung von Betriebszyklen bei solarthermischen Kraftwerken mit Flüssigsalzen als Wärmeträgermedien,” 2012.
[5] C. Odenthal, W.-D. Steinmann, M. Eck, and D. Laing, “The CellFlux Storage Concept for Cost Reduction in Parabolic Trough Solar Thermal Power Plants,” *Energy Procedia*, vol. 46, pp. 142–151, 2014.
[6] K. G. Allen, “Rock bed thermal storage for concentrating solar power plants,” 2014.
[7] C. Odenthal, W.-D. Steinmann, and M. Eck, “Simulation and experimental results of the CellFlux storage concept,” *Eurotherm Semin. #99*, no. 99, pp. 1–12, 2014.